

## II. MICROWAVE GASEOUS DISCHARGES\*

Prof. S. C. Brown	Dr. L. Mower	W. R. Kittredge
Prof. W. P. Allis	R. R. Brown II	J. J. McCarthy
Prof. D. O. Akhurst	C. D. Buntschuh	R. G. Meyerand, Jr.
Prof. D. R. Whitehouse	S. Frankenthal	W. J. Mulligan
Dr. G. Bekefi	R. B. Hall	Judith L. Shaver
Dr. S. J. Buchsbaum	J. L. Hirshfield	C. S. Ward

### A. MICROWAVE NOISE RADIATION FROM PLASMAS

Microwave noise power generated by a plasma of low degree of ionization (less than 0.1 per cent) results from free-free electron-molecule collisions with a subsequent emission of a photon. It is generally stated that the noise power is given by the simple relation  $P = kT_e \Delta f$ , where  $k$  is Boltzmann's constant,  $T_e$  the electron temperature, and  $\Delta f$  the bandwidth of the receiver. Previous experimental evidence (1, 2) obtained from studies of the radiation from the positive column of dc discharges indicates that this formula is approximately valid in the range of currents and gas pressures that have been studied.

We have undertaken a series of noise measurements in dc helium discharges over a large range of plasma parameters. A sensitive radiometer (3) of 2 mc bandwidth, operating at 3000 mc and capable of measuring power levels of  $10^{-16}$  watt, was used for this purpose. This sensitivity was attained by periodic switching at a rate of 30 cps between the unknown noise source situated in one waveguide and a fixed standard noise source situated in a second waveguide. The difference between the power outputs was detected synchronously at the switching rate. Precision attenuators placed adjacent to the two noise sources were adjusted for a null reading of the detector. The discharge was produced in a cylindrical Pyrex tube, 1 inch in diameter and 16 inches long, between a hot oxide-coated cathode and a water-cooled anode.

Typical measurements are shown in Fig. II-1. On the abscissa the electron density obtained from (a) the voltage current characteristics of the discharge, and (b) microwave transmission measurements made in a cavity surrounding a section of the plasma column is plotted. The  $TE_{011}$  mode of a cylindrical cavity resonant at 4300 mc was used. On the ordinate the noise power radiated by the discharge relative to the noise emitted by the standard source is plotted. The power emission from the standard was that of a noise source at an equivalent temperature of approximately 10,500° K. Each curve represents a different gas pressure  $p_0$  normalized to 0° C.

Note that the power emitted increases nearly linearly with electron density up to values of approximately  $3 \times 10^{10}$  electrons/cc. At values of approximately  $10^{12}$  electrons/cc the power output saturates. It is this "plateau" region that has been mainly studied in the past. Here the plasma radiates well-nigh as a black body over the

---

\*This work was supported in part by the Atomic Energy Commission under Contract AT(30-1)1842.

## (II. MICROWAVE GASEOUS DISCHARGES)

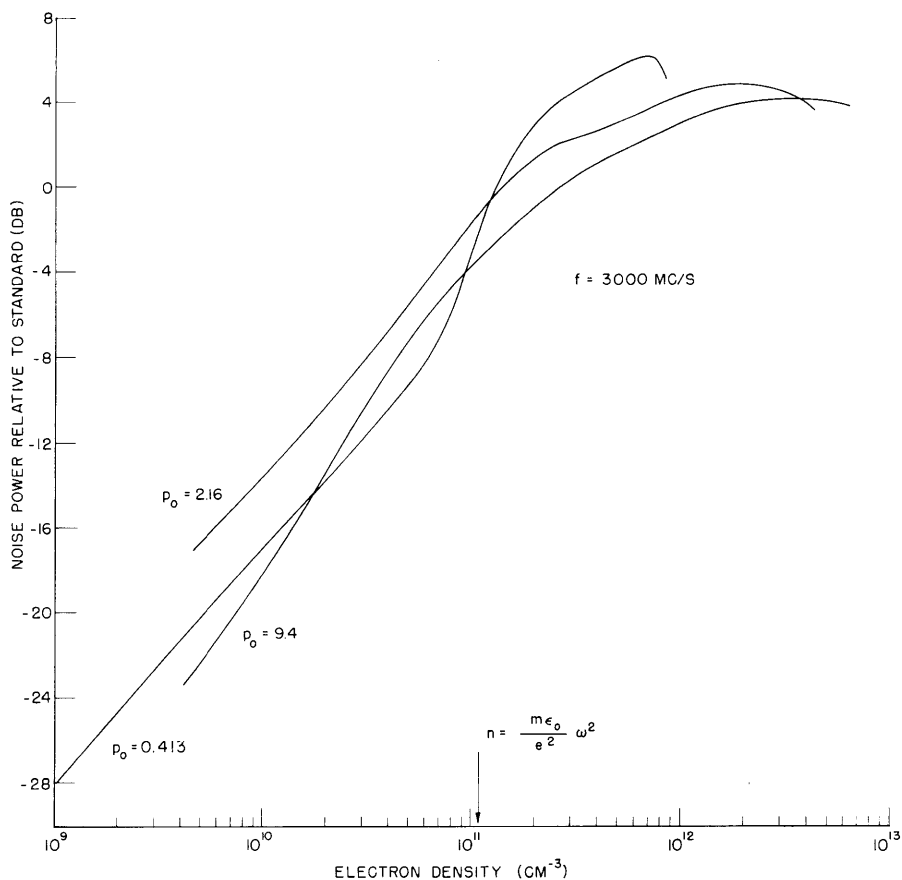


Fig. II-1. Microwave noise power as a function of electron density for several gas pressures. ( $p_0$  in mm Hg normalized to 0° C.)

frequency range that we observed. At lower electron densities, in the neighborhood of and below that corresponding to the plasma frequency ( $1.1 \times 10^{11}$  electrons/cc), the aforementioned formula for the noise power output fails. In this range the degree of opacity of the plasma with respect to the emerging radiation must be considered. Preliminary calculations, with the use of the attenuation sustained by an electromagnetic wave in traversing the plasma (4, 5), explain the general trend of the curves. The rather sharp fall-off in noise output observed at the low gas pressures (see the 0.216 mm Hg curve of Fig. II-1) that occurs at approximately  $10^{11}$  electrons/cc is believed to be caused by the known rapid increase of the attenuation coefficient in the vicinity of the plasma frequency. Quantitative comparison of experiment with theory is being made.

When a plasma is permeated by a dc magnetic field directed along the length of the plasma column, the noise radiation is greatly changed. In particular, preliminary measurements indicate enhancement of noise radiation when the electron density is adjusted to values at which the real and the imaginary parts of the plasma

## (II. MICROWAVE GASEOUS DISCHARGES)

propagation coefficient pass through strong maxima. Further studies of radiation from magnetized plasmas are planned.

G. Bekefi, J. L. Hirshfield

### References

1. W. W. Mumford, Bell System Tech. J. 28, 608 (1949).
2. K. S. Knol, Philips Res. Rep. 6, 288 (1951).
3. J. P. Wild, Observational radio astronomy, Advances in Electronics and Electron Physics, Vol. VII (Academic Press, Inc., New York, 1955), p. 299.
4. S. J. Buchsbaum, Interaction of electromagnetic radiation with a high density plasma, Ph.D. Thesis, Department of Physics, M.I.T., 1957.
5. L. Nedelsky, Phys. Rev. 42, 641 (1932).

## B. ELECTROMAGNETIC CONTAINMENT OF CHARGED PARTICLES

It has been shown that it is possible to exert confining forces on charged particles in a microwave cavity (1,2). If such a confining force could be exerted on the electrons in a gas discharge, it would be possible to maintain the plasma at a higher temperature because the loss of particles by diffusion would be decreased. This report indicates some of the properties of a particular cavity that was used for containment.

The confining force on an electron is the time-averaged sum of both the Lorentz force and the strong-focusing force. The resultant force, according to first-order theory, is

$$\bar{f} = \frac{-e^2}{4\omega^2 m} \nabla E^2 \quad (1)$$

When the force on a particle is the gradient of a scalar potential, as indicated by Eq. 1, the sum of kinetic and potential energies is a constant.

$$\frac{1}{2} \frac{m}{e} \left( v_i^2 - v^2 \right) = \frac{e}{4\omega^2} \left( E^2 - E_i^2 \right) \quad (2)$$

The subscript i in Eq. 1 represents the initial conditions. One of the simplest of the field configurations that exerts confining forces toward a single region of space is the  $TM_{011}$  mode in a cylindrical cavity. The electric field of this mode is given by

$$E = E_0 \left[ \bar{i}_r J_1(pr) \cos B_z z - \bar{i}_z \frac{p}{B} J_0(pr) \sin Bz \right] \quad (3)$$

L = length of cavity

a = radius of cavity

where  $B = \pi/L$ ,  $p = (2.405)/a$ . This electric field is zero at the origin and increases

(II. MICROWAVE GASEOUS DISCHARGES)

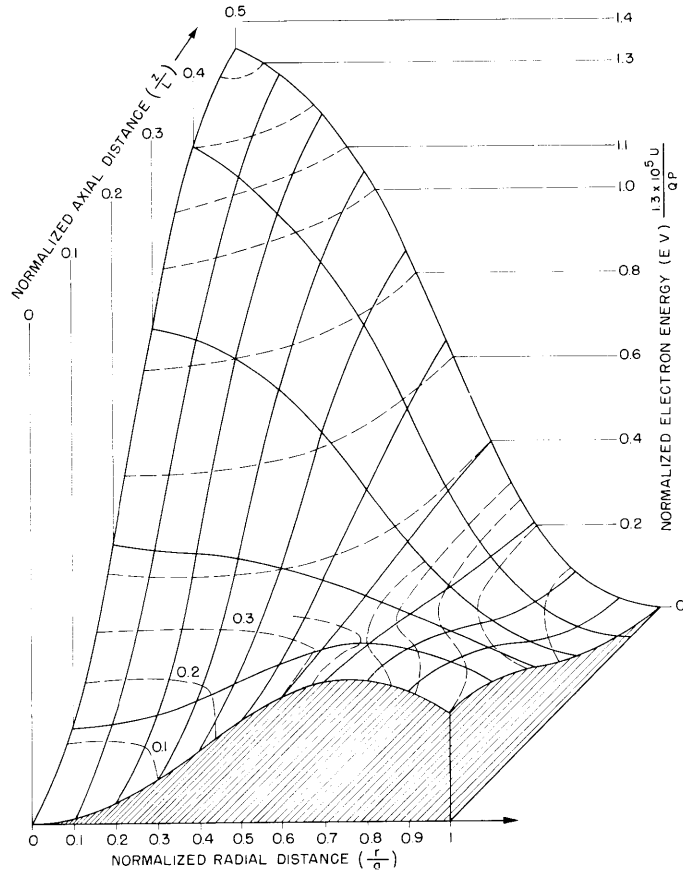


Fig. II-2. Potential hill diagram of  $TM_{011}$  cavity for containment.

in magnitude in all directions from the origin. From Eq. 1 it can be seen that a particle has oscillatory motion about the origin. If the amplitude of the particle motion is small, the electric field, as given by Eq. 3, can be represented by linear terms.

$$E = E_0 p \left[ \frac{r}{2} \bar{i}_r - z \bar{i}_z \right] \quad (4)$$

From Eqs. 2 and 4 an expression for the ratio  $[(\omega X_{\max})/V_i]$  can be formed. This ratio is the product of the frequency and the maximum amplitude of motion divided by the initial velocity. It is desirable to minimize this quantity when the power input to the cavity and the Q of the cavity are fixed. The only parameter that can be varied is the ratio of length to radius of the cavity. When this optimization is carried out,

$$\left. \frac{P^2}{B^2} \right|_{\text{opt}} = \frac{4}{3} \quad (5)$$

is obtained. When the condition represented by Eq. 5 is fulfilled, the ratio  $[(\omega X_{\max})/V_i]$

## (II. MICROWAVE GASEOUS DISCHARGES)

is minimum only for small amplitude oscillations.

It is necessary to indicate what electron energies can be contained in the  $TM_{011}$  cavity, which has been constructed according to the condition of Eq. 5. From Eq. 2, a particle starting from the origin must stay within bounds in the cavity so that

$$U_i < \frac{\frac{e}{m} E^2}{4\omega^2} \quad (6)$$

Figure II-2 indicates contours of constant energy in the  $TM_{011}$  cavity; only one quadrant of the  $r$ - $z$  plane is shown.

A 1000-watt magnetron will be used to contain a gas discharge in a cavity. The electron energies that can be contained may be found from Fig. II-2. If we assume a  $Q$  of  $10^4$ , the maximum energy that can be contained is  $V_i = 24.6$  ev. This energy corresponds to the lowest barrier on the potential hill of  $(1.3 \times 10^5 U)/QP = 0.32$ .

R. B. Hall

### References

1. H. A. H. Boot, S. A. Self, and R. B. R. Shersby-Harvie, Containment of a fully ionized plasma by radio frequency fields, *J. Electronics and Control*, pp. 434-453, May 1958.
2. M. L. Good, A proposed particle containment device, Report 4146, University of California Radiation Laboratory, Berkeley, California, July 8, 1953.

## C. THE INTERACTION OF A PLASMA BEAM WITH A MAGNETIC FIELD

The interaction of a plasma beam with a magnetic field has been studied with the use of the apparatus shown in Fig. II-3.

### 1. Plasma Beam Production

The plasma beam is produced by a high-current ion source that was described in the Quarterly Progress Report of October 15, 1957, page 9. The beam density can be varied from  $10^6$  to  $10^{11}$  ions per cubic centimeter. The energy of the ions in the plasma beam can be varied from a few hundred to a few thousand electron-volts. When a low current, and consequently a low-density ion beam, is produced, the densities of electrons and ions in the beam are not necessarily equal. However, when the beam density is increased to above  $10^8$  ions/cm<sup>3</sup>, the space charge of the ions will trap electrons in the beam and produce space-charge neutralization. The energies and velocities of the two particles, ions and electrons, need not be equal. Thus we could have a plasma beam that has a finite current and also equal charge densities.

## (II. MICROWAVE GASEOUS DISCHARGES)

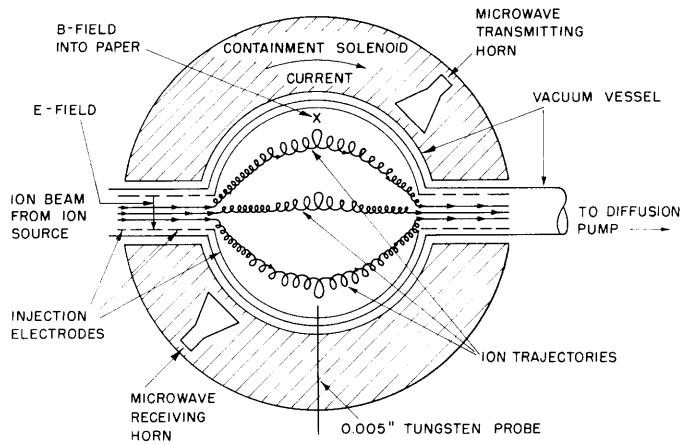


Fig. II-3. Schematic view of experiment.

### 2. Plasma Diagnostics

The plasma produced in the magnetic field is detected by three means:

(a) A small tungsten wire (5-mil diameter) acts as a probe in the plasma, and current collected by this wire serves to measure the plasma density.

(b) S-band microwave power is transmitted through the plasma. The transmission path serves as one arm of a bridge that is unbalanced because of the presence of the plasma and also measures the plasma density.

(c) The diamagnetic effect of the plasma is used to measure the product of the plasma density and plasma energy. The diamagnetic effect has been treated fully by W. P. Allis and S. J. Buchsbaum (1).

### 3. Interaction of the Plasma Beam with a Magnetic Field

The first set of experiments deals with the behavior of the plasma beam when the density of particles is sufficiently low that space-charge forces are unimportant; that is,  $10^8$  to  $10^6$  particles per cubic centimeter. The second set of experiments deals with the high-density case; that is, when the density of the ion beam is higher than  $10^8$  ions per cubic centimeter.

### 4. Low-Density Beam Interaction

Figure II-4 shows the plasma densities that result when a low-current beam of ions is directed toward the magnetic field. The densities of ions and electrons (assumed to be equal) is plotted against the electric field produced by the external electrodes, as shown in Fig. II-3. The parameter for the family of curves is the magnetic field produced by the confining solenoid  $B_0$ . The application of an electric field by the electrodes produces, first, an initial increase in the plasma density and then leads to a decrease. As

## (II. MICROWAVE GASEOUS DISCHARGES)

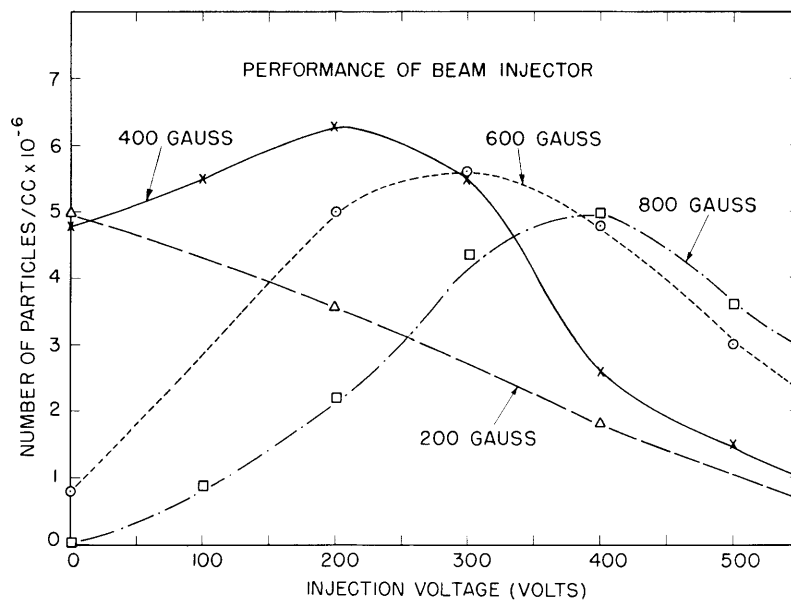


Fig. II-4. Results of beam injection into magnetic field.

the magnetic field is increased, the maximum plasma density moves progressively to higher electric fields for higher magnetic fields. This behavior is explained rather completely by looking at a single-particle model. A single ion enters the magnetic field, experiences a  $V \times B$  force which tends to bend its trajectory, and also sees an electrostatic force  $eE$  which is directed in the opposite direction. If the magnetic force is greater than the electric force, the ion will take on a curved trajectory and will hit the inside of the vacuum vessel before it has a chance to reach the inside of the plasma containment vessel. As the electric field is increased, the path becomes a straight line, and for a certain optimum electric field, the greatest number of ions will have straight-line trajectories and the greatest plasma density will be produced. As the electric field is increased still more, it will begin to overbalance the magnetic deflecting force, and the ions will curve in the opposite direction, once again intersecting the vacuum vessel. The component of the electric field perpendicular to the magnetic field divided by the magnitude of the magnetic field gives the velocity of the particles. The velocity of the ions determined by this method is in good agreement with the velocities observed for ions in the plasma beam itself. Also, as the magnetic field is increased, this ratio should stay constant. Figure II-4 shows that this is roughly the case. The densities shown in Fig. II-4 were calculated from the current drawn from the probe in the plasma containment region. This was done because the probe has the greatest sensitivity and allows the observation of plasmas of densities below  $10^6$  particles per cubic centimeter. However, when the beam density was increased, the plasma density was allowed to approach  $10^8$  particles per cubic centimeter, and the data obtained both from the microwave

## (II. MICROWAVE GASEOUS DISCHARGES)

transmission apparatus and from the diamagnetic apparatus agreed with the probe current.

The particle trajectories for the low-density case are shown in Fig. II-3. In the plasma containment region the ions move in a cycloidal path, which means that the ions will have energy in rotation, in addition to their linear translation. This is the desirable situation, since we now have a chance of allowing the particles to collide head-on with the full kinetic energy of the beam and produce an isotropic energy distribution in the plasma.

### 5. High-Density Beam Interaction

Figure II-5 shows the results of injecting progressively higher beam densities into the containing magnetic field. Again, as the electric field is increased, the plasma density increases up to an optimum electric field and then decreases. However, the maximum observed for an optimum electric field becomes much less pronounced, and for the highest beam density observed, approximately  $1 \times 10^{11}$  particles per centimeter, the increase has almost entirely disappeared. Thus some mechanism must be postulated to explain the behavior of the plasma beam which will allow it to enter a static magnetic field without the assistance of an external electric field.

Figure II-6 shows a beam configuration that would produce this behavior. The plasma beam enters the magnetic field and the Lorentz  $V \times B$  forces begin to act on the ions and electrons, deflecting them in opposite directions. However, since the density is high, the numbers of ions and electrons deflected are sufficiently great that a large electrostatic force develops between the charged particles. Thus the beam becomes polarized because of charge separation, and the electrostatic force grows in magnitude until it is

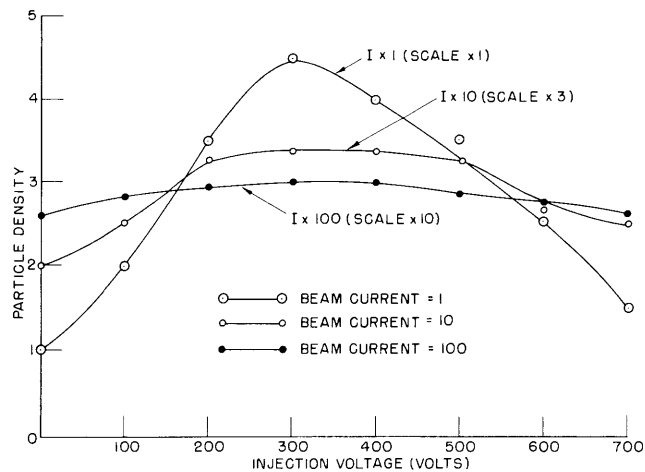


Fig. II-5. Effect of higher beam currents on plasma density.



## (II. MICROWAVE GASEOUS DISCHARGES)

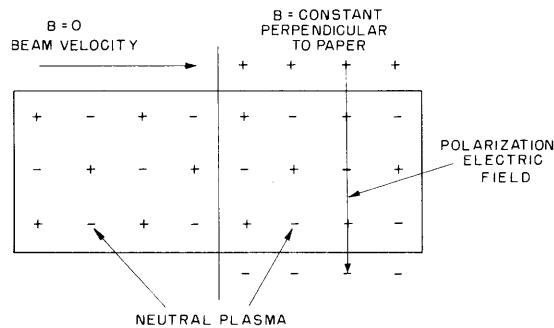


Fig. II-6. Beam polarization in magnetic field.

equal to the magnetic force. Therefore, the beam divergence stops and no more particles can be withdrawn from the beam, since the electrostatic force will stop their deflection by the magnetic field. A simple calculation shows that the electric field that is produced is exactly equal to  $V \times B$ , which was the optimum electric field found for the low-density injection case. Thus the plasma beam will produce its own electric field, which is necessary for its transit across the magnetic field. This, of course, is greatly at odds with a single-particle model in which the ions and electrons would simply be deflected in opposite directions and can only be explained by taking into account the forces between the charged particles.

When the plasma-detection techniques that have been described were used, it was found that the plasma density in the plasma containment region was approximately 1/10 to 1 per cent of the density in the plasma beam. Thus very little plasma is being produced for a reasonably high density beam. This is explained by the fact that when the plasma beam can produce its own electric field and cross the magnetic field, it will stay roughly in the form of a beam, and very few of the particles will take on the desired cycloidal path and remain trapped in the magnetic field.

Another experiment was performed to verify the fact that the plasma beam is really crossing the magnetic field. The electrodes at the far end of the plasma containment region were grounded, and the current flowing to them was measured. It was determined that a sizable fraction of the total beam current, approximately 5 per cent, was reaching these plates. The distance from these collecting plates and the region where the ions enter the magnetic field is approximately ten times the Larmor radius of the ions. The presence of ions at a position where a single-particle model would rule out their existence can only be accounted for by the action of an electric field produced by beam polarization which would allow the beam to cross the magnetic field.

The remaining 95 per cent of the beam is lost because the ions have a very broad velocity spectrum in the beam. The electric field in the beam, of course, can only have one unique value at every point. For this value of electric field, only one particular

## (II. MICROWAVE GASEOUS DISCHARGES)

velocity of ion will have a straight-line trajectory. Those with higher velocities than the optimum velocity will be deflected as will also those with lower velocities. Thus particles are gradually lost from the beam and will hit the walls of the plasma containment region. A calculation of the number of particles lost as the beam traverses the magnetic field is in rough agreement with the 5 per cent of the beam current found at the distance specified in the experiment.

R. G. Meyerand, Jr.

### References

1. W. P. Allis and S. J. Buchsbaum, Diamagnetism of a long cylindrical plasma, Quarterly Progress Report, Research Laboratory of Electronics, M.I.T., July 15, 1958, p. 5.

### D. EFFECT OF IONS ON RF CONDUCTIVITY OF A MAGNETIZED PLASMA

A bridge network capable of measuring the impedance of a coil loaded with a coaxial plasma has already been reported (1). It was pointed out that experimental conditions are such that the plasma ions can contribute significantly to, and indeed dominate, the transport properties of the plasma (2). In this report we show the effect of the plasma on the impedance of the coil, taking account of ions, as well as of proper boundary conditions at the edge of the plasma.

The change in the complex impedance of the coil is related to the quantity  $(\vec{J}^* \cdot \vec{E})$  integrated over the volume of the plasma, where  $\vec{J}$  and  $\vec{E}$  are the total rf current and field in the plasma. Care must be taken in evaluating the quantity  $(\vec{J}^* \cdot \vec{E})$  because in the magnetized plasma, in addition to the azimuthal component of the E-field which is induced by the coil, there exists a radial Hall field. The radial current, however, is negligibly small because of the low frequency that is used ( $f = 1$  mc) and because the glass envelope prohibits the flow of conduction current in the radial direction. As a result, at plasma electron densities greater than  $10^7$  cm<sup>-3</sup>, with the total conduction current much larger than the total displacement current, it is a good approximation to set  $J_{\text{radial}} = 0$ . Under these conditions, it is somewhat more convenient to calculate the quantity  $(\vec{J}^* \cdot \vec{E})$  by using the plasma resistivity tensor  $\underline{\underline{R}}$ , since  $(\vec{J}^* \cdot \vec{E}) = |\vec{E}_\theta|^2 / R_{\theta\theta}$ , where

$$\underline{\underline{R}} = \begin{pmatrix} R_{rr} & R_{r\theta} & 0 \\ R_{\theta r} & R_{\theta\theta} & 0 \\ 0 & 0 & R_{zz} \end{pmatrix} = (\underline{\underline{\sigma}})^{-1} = \begin{pmatrix} \sigma_{rr} & \sigma_{r\theta} & 0 \\ \sigma_{\theta r} & \sigma_{\theta\theta} & 0 \\ 0 & 0 & \sigma_{zz} \end{pmatrix}^{-1}$$

(II. MICROWAVE GASEOUS DISCHARGES)

$$\begin{aligned}
 \sigma_{r\theta} &= -\sigma_{\theta r} & R_{rr} &= R_{\theta\theta} = \frac{\sigma_{rr}}{\sigma_{rr}^2 + \sigma_{r\theta}^2} \\
 \sigma_{rr} &= \sigma_{\theta\theta} & R_{r\theta} &= -R_{\theta r} = \frac{-\sigma_{r\theta}}{\sigma_{rr}^2 + \sigma_{r\theta}^2} \\
 R_{zz} &= \frac{1}{\sigma_{zz}}
 \end{aligned} \tag{1}$$

The transverse diagonal components of the resistivity tensor give the magnetoresistance coefficient of the plasma and the off-diagonal components give the Hall coefficient. The components of the tensor must, of course, include the effect of the ions. This is accomplished by writing for the conductivity tensor, after Allis (3),

$$\underline{\sigma} = \frac{ne^2}{2m} \begin{pmatrix} \ell + r & j(\ell - r) & 0 \\ -j(\ell - r) & \ell + r & 0 \\ 0 & 0 & 2p \end{pmatrix} + \sum_i \frac{N_i e^2}{2M_i} \begin{pmatrix} L_i + R_i & j(L_i - R_i) & 0 \\ -j(L_i - R_i) & L_i + R_i & 0 \\ 0 & 0 & 2P_i \end{pmatrix}$$

where

$$\begin{aligned}
 \left. \begin{matrix} \ell \\ r \end{matrix} \right\} &= \frac{1}{\nu_{c-} + j(\omega \pm \omega_{b-})} & p &= \frac{1}{\nu_{c-} + j\omega} & \omega_b &= \left| \frac{eB}{m} \right| \\
 \left. \begin{matrix} L_i \\ R_i \end{matrix} \right\} &= \frac{1}{\nu_{c_{i+}} + j(\omega \mp \omega_{b_{i+}})} & P_i &= \frac{1}{\nu_{c_{i+}} + j\omega} & \omega_{b_i} &= \left| \frac{eB}{M_i} \right|
 \end{aligned} \tag{2}$$

and where the summation is over all ionic species. In Eqs. 2 all collision frequencies  $\nu_c$  are assumed to be independent of the particle velocity.

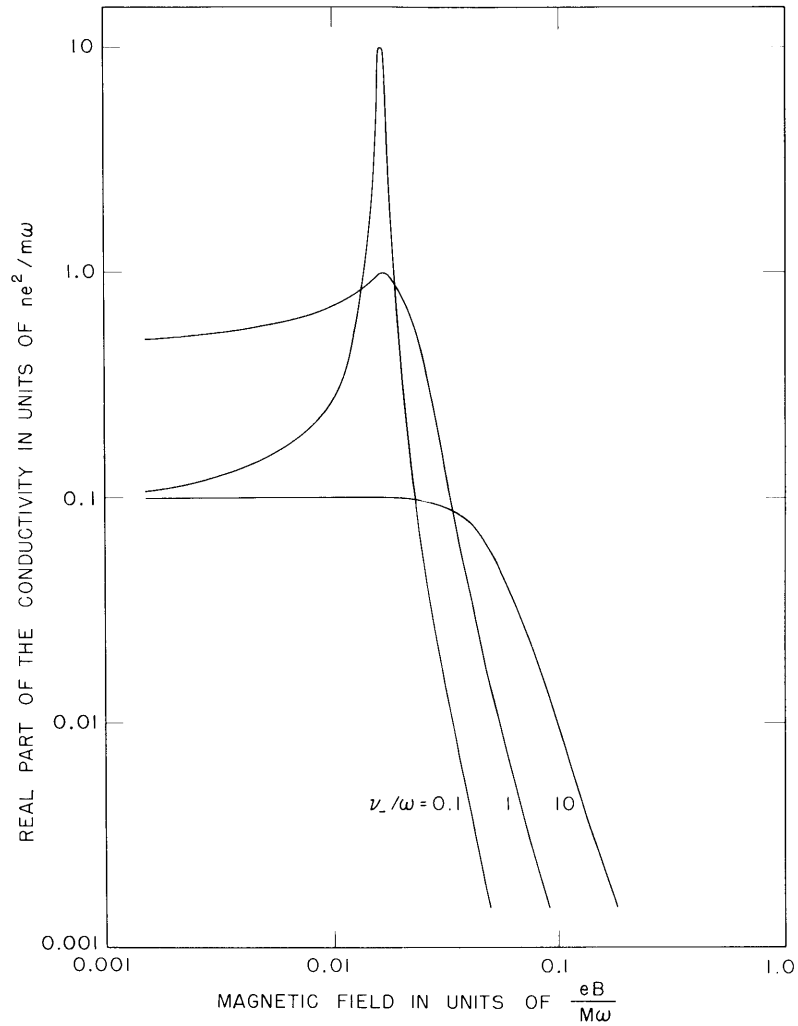
In the present discussion we limit ourselves to a neutral plasma with a single ion species. The conductivity tensor can then be written

$$\underline{\sigma} = \frac{ne^2}{2m} \begin{pmatrix} [(\ell+r) + f(L+R)] & j[(\ell-r) + f(L-R)] & 0 \\ -j[(\ell-r) + f(L-R)] & [(\ell+r) + f(L+R)] & 0 \\ 0 & 0 & 2(p+fP) \end{pmatrix} \tag{3}$$

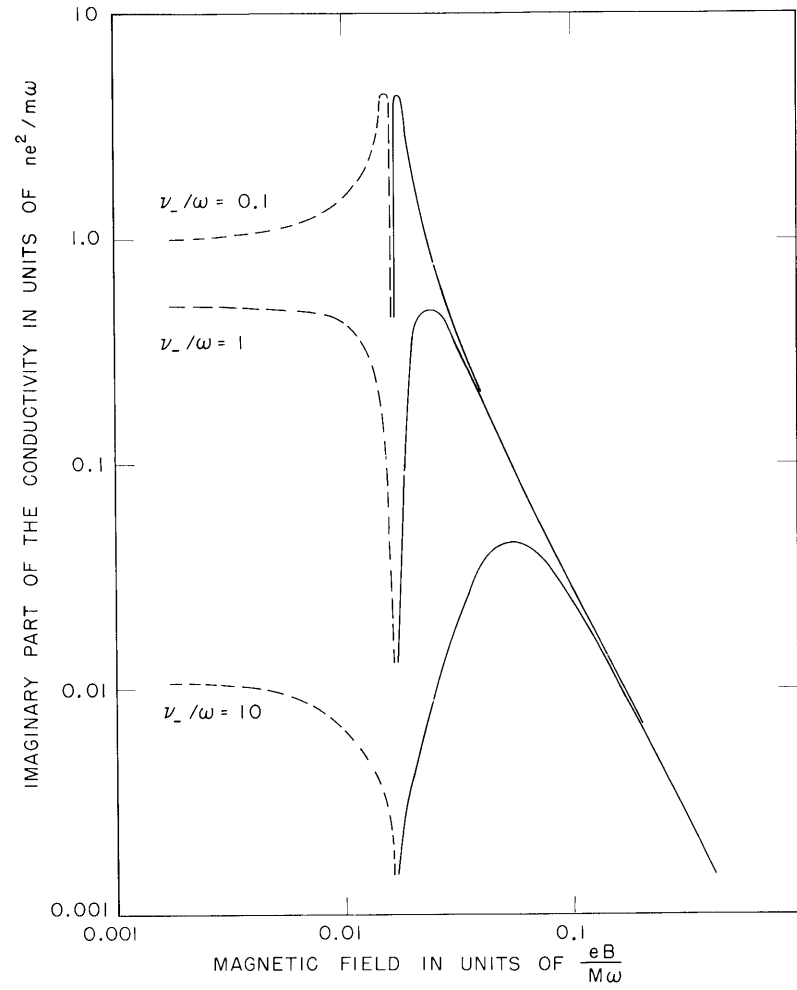
where  $f = m/M$ . The diagonal resistivity component  $R_{\theta\theta}$  is

$$R_{\theta\theta} = \frac{m}{2ne^2} \left[ \frac{1}{\ell + fL} + \frac{1}{r + fR} \right] \tag{4a}$$

$$= \frac{m}{ne^2} \left[ \frac{\left\{ (\nu_{c-} - \nu_{c+}) - (\omega^2 - \omega_{b+} \omega_{b-}) \right\} + j\omega(\nu_{c+} + \nu_{c-})}{(\nu_{c+} + f\nu_{c-}) + j\omega(1+f)} \right] \tag{4b}$$



(a)



(b)

Fig. II-7. (a) Real and (b) imaginary parts of the effective conductivity ( $1/R_{\theta\theta}$ ) as functions of the magnetic field (dashed lines refer to negative values of conductivity).

## (II. MICROWAVE GASEOUS DISCHARGES)

Note that for vanishingly small  $\nu_{c-}$  and  $\nu_{c+}$ ,  $R_{\theta\theta}$  goes through zero at  $\omega = (\omega_{b-}\omega_{b+})^{1/2}$ ; that is, there is a resonance at the geometric mean of the electron and ion cyclotron frequencies. There is no resonance at either  $\omega_{b-}$  or  $\omega_{b+}$ . The reason for this lies in the induced radial Hall field (and the lack of radial current) which tightly couples the electron and ion motions and results in the hybrid resonant frequency  $\omega = (\omega_{b-}\omega_{b+})^{1/2}$ . Figure II-7a and b shows the real and imaginary parts of  $1/R_{\theta\theta}$ , computed from Eq. 4b, in the vicinity of the resonance for  $H_2^+$  ions; the ratio  $\nu_{c-}/\nu_{c+}$  was assumed to be equal to 100.

This formulation is not exact in that no way is shown for calculating the net rf space charge  $\rho$ . From the condition  $J_r = 0$  and the conductivity equation, it follows that  $\rho$  is zero, but the finite Hall field

$$\left( E_r = \frac{R_{r\theta}}{R_{rr}} E_\theta = -\frac{\sigma_{r\theta}}{\sigma_{rr}} E_\theta \right)$$

implies a finite space charge. The difficulty is eliminated if we include the displacement current and treat the problem exactly with the aid of Maxwell's equations.

$$\nabla \cdot \vec{E} = \rho/\epsilon_0 \quad (5a)$$

$$\nabla \times \vec{E} = -j\omega\mu_0 \mathbf{B} \quad (5b)$$

$$\nabla \times \vec{H} = j\omega\epsilon_0 \vec{E} + \vec{\sigma} \cdot \vec{E} = j\omega\epsilon_0 \vec{K} \cdot \vec{E} \quad (5c)$$

where  $\vec{K} = 1 + \vec{\sigma}/j\omega\epsilon_0$  is the effective dielectric coefficient tensor of the plasma. Equation 4a and the continuity equation can be combined to give

$$\nabla \cdot (\vec{K} \cdot \vec{E}) = 0 \quad (6)$$

Experimental conditions are such that  $\frac{\partial}{\partial \theta} = \frac{\partial}{\partial z} = 0$  (fringing fields are neglected). Equation 6 then yields the Hall field

$$E_r = -\frac{K_{r\theta}}{K_{rr}} E_\theta = -\frac{\sigma_{r\theta}}{j\omega\epsilon_0 + \sigma_{rr}} E_\theta \quad (7)$$

Using Eq. 7 in Eq. 5c, we obtain an equation for  $E_\theta$

$$(\nabla \times \vec{H})_\theta = j\omega\epsilon_0 \left( K_{\theta\theta} - \frac{K_{\theta r} K_{r\theta}}{K_{rr}} \right) E_\theta \quad (8a)$$

$$= j\omega\epsilon_0 K_{\text{eff}} E_\theta \quad (8b)$$

where

## (II. MICROWAVE GASEOUS DISCHARGES)

$$K_{\text{eff}} = K_{\theta\theta} - \frac{K_{\theta r} K_{r\theta}}{K_{rr}} \quad (9)$$

The expression  $(\vec{J}^* \cdot \vec{E})$  is given by

$$(\vec{J}^* \cdot \vec{E}) = (j\omega\epsilon_0 \vec{K} \cdot \vec{E})^* \cdot \vec{E} = -j\omega\epsilon_0 K_{\text{eff}}^* |E_\theta|^2 \quad (10)$$

Equation 10 yields results that are not significantly different from those given by  $(\vec{J}^* \cdot \vec{E}) = |E_\theta|^2 / R_{\theta\theta}$  when the plasma electron density is larger than  $10^7 \text{ cm}^{-3}$ . However, the exact formulation yields uniquely the rf space charge  $\rho$

$$\rho/\epsilon_0 = -\frac{1}{r} \frac{\partial}{\partial r} r \left[ \frac{\sigma_{r\theta}}{j\omega\epsilon_0 + \sigma_{rr}} E_\theta \right] \quad (11)$$

It should be pointed out that although rf space-charge fields are properly taken into account, dc radial space-charge fields (which must exist in any high-density plasma column) are not considered. The presence of a dc field affects, in general, the rf motion of an ion in a magnetized plasma. Thus it affects the impedance of the coil (4). The general effect is to broaden, or even obliterate, the hybrid resonance.

S. J. Buchsbaum

### References

1. J. W. Graham and R. S. Badessa, Ion cyclotron resonance measurement system, Quarterly Progress Report, Research Laboratory of Electronics, M.I.T., April 15, 1958, p. 7.
2. S. J. Buchsbaum, Ion cyclotron resonance, Quarterly Progress Report, op. cit., p. 5.
3. W. P. Allis, Motions of ions and electrons, Handbuch der Physik, Vol. 21 (Springer Verlag, Berlin, 1956), p. 413.
4. Detailed calculations of the effects of dc space charge are now being made.

### E. MICROWAVE PROPERTIES OF WARM, ANISOTROPIC PLASMAS

Several investigations (1) of the microwave properties of anisotropic plasmas which have sought to include the effects of nonzero electron and ion temperature have recently been reported. In these treatments the electric conductivity and/or the electromagnetic propagation constant are calculated for macroscopically uniform, electrically neutral plasmas in the presence of a uniform dc magnetic field. In all cases the plasma is found to be a dispersive medium not only as a function of the usual variables but also as a function of the wavelength of the electromagnetic field within the plasma. The form of the conductivity tensor differs, however, in the different treatments of the problem.

It is the purpose of this investigation to determine the nature of these differences and

## (II. MICROWAVE GASEOUS DISCHARGES)

to note the similarities. The results indicate that the treatment of Bernstein is correct for propagation at an arbitrary angle relative to the imposed dc magnetic field. In the absence of collisions, the treatment of Drummond agrees with Bernstein's treatment only for the specific cases of propagation parallel or transverse to the dc magnetic field. The details of our analysis will appear later.

L. Mower

### References

1. A. G. Sitenko and K. N. Stepanov, *Zh. eksper. teor. Fiz.* 31, 642 (1956); T. Pradhan, *Phys. Rev.* 107, 1222 (1957); I. B. Bernstein, *Phys. Rev.* 109, 10 (1958); J. E. Drummond, *Phys. Rev.* 110, 293 (1958).